Research Article

Journal of RAMAN SPECTROSCOPY

Received: 22 June 2009 Accepted: 18 September 2009 Published online in Wiley Online Library: 18 November 2009

(wileyonlinelibrary.com) DOI 10.1002/jrs.2530

# Structural analysis of $x$CsCl(1 − $x$)$Ga_2S_3$ glasses by means of DFT calculations and Raman spectroscopy

Arnaud Cuisset,[a]* Francis Hindle,[a] Jacky Laureyns[b] and Eugène Bychkov[a]

**The alkali metal halide doping of gallium-sulfide glasses yields improvements in the optical, thermal and glass forming properties. To understand these improvements, the short-range order of $x$CsCl(1 − $x$)$Ga_2S_3$ glasses was probed by Raman spectroscopy. Raman spectra have been interpreted using density functional theory (DFT) harmonic frequency calculations on specific clusters of $GaS_4H_4$ and/or $GaS_3H_3Cl$ tetrahedral subunits. The assignment of the observed vibrational bands confirms the main structural conclusions obtained with X-ray and neutron diffraction experiments and gives some new insights into the gallium-network present in the $x$CsCl(1 − $x$)$Ga_2S_3$ glasses. At the lowest concentration, the observed spectrum may be interpreted with small clusters such as dimers and trimers connected by corner-sharing (CS) $GaS_4H_4$ tetrahedral subunits. The vibrational fingerprints of tri-clusters with three-fold coordinated sulfur atoms have also been identified; however, no Raman signature of chlorine-doped subunits has been found to be caused by their insufficient intensity. For higher CsCl concentrations, distinct spectral features corresponding to chlorine-doped clusters appear and are increasing in intensity with $x$. In other words, undoped and Cl-doped tetrahedra coexist in the $x$CsCl(1 − $x$)$Ga_2S_3$ glasses. The added chlorine atoms induce a fragmentation of the glass network and replace the sulfur atoms in the CS tetrahedral environment. The comparison of the observed spectra with theoretical predictions and diffraction data favoured one-fold coordinated chlorine atoms in the glass network.** 

**Keywords:** chalcogenide glasses; chalcohalide glasses; Raman spectroscopy; DFT calculations; short-range structure

## Introduction

Owing to their low phonon density of states and high quantum efficiency, rare-earth-doped sulfide glasses have been extensively used for photonic applications such as fibre optical amplifiers, up-converters and fibre-lasers.[1] Alkali metal halide-substituted gallium-sulfide glasses have demonstrated high quantum efficiencies combined with improved thermal and glass forming properties compared with the unsubstituted glass.[2,3] The key to understand these improvements may lie in the knowledge of the short-range molecular structure of the gallium-sulfide network and of the structural modifications produced by the alkali doping. High-energy X-ray diffraction and neutron diffraction are powerful tools for the structural analysis of glasses. The analysis of the information collected with these techniques allows the average short-range structure to be determined. Nevertheless, additional experimental techniques such as vibrational spectroscopy allow further information to be obtained. With these experimental techniques, structural details are increased and the local configurations of the amorphous network could be revealed. Numerous studies using Infrared and/or Raman spectroscopies supplemented by quantum mechanical investigations demonstrate their abilities to obtain relevant structural information on clusters which have been identified in glass materials.[4–9] The observed vibrational resonances may be assigned by comparison to the theoretical spectra allowing a quantitative determination of specific clusters present in the glass. Using *ab initio* and semi-empirical calculations, Grisolía *et al*. 2006 performed a geometrical study of $Ga(SCH_3)_4$ and $Ga(SCH_3)_3Cl$ and their corner-sharing (CS) and edge-sharing (ES) dimers, comparing the theoretical predictions with structural conclusions obtained by X-ray absorption spectroscopy (XAS).[4,10] The calculated differences between the Ga–S bond lengths show that XAS may not allow an unambiguous differentiation between the chlorine-doped and undoped clusters. Grisolía *et al*. 2006 conclude that vibrational spectroscopy techniques are required to understand the organisation of the gallium sulfide tetrahedral structure and the role of chlorine atoms in the glass network. The calculated harmonic frequencies highlighted that infrared spectroscopy is very well suited to probe chlorine substitutions and to differentiate between the vibrational fingerprints of the CS and ES dimers. The vibrational transitions observed in Raman spectra may be also interpreted in a frame of structural models assumed for the chalcogenide/halide glasses in comparison with reference compounds.[11] Unfortunately, no vibrational spectroscopic experiments have been completed over the whole composition range for these systems. Therefore, in the present work, the experimental Raman spectra obtained for different CsCl concentrations are compared with theoretical spectral

* *Correspondence to: Arnaud Cuisset, Laboratoire de Physico-Chimie de l'Atmosphère CNRS UMR 8101, Bâtiment MREI2, Université du Littoral Côte d'Opale, 189A avenue Maurice Schumann, 59140 Dunkerque, France. E-mail: arnaud.cuisset@univ-littoral.fr*

a *Laboratoire de Physico-Chimie de l'Atmosphère CNRS UMR 8101, Bâtiment MREI2, Université du Littoral Côte d'Opale, 189A avenue Maurice Schumann, 59140 Dunkerque, France*

b *Laboratoire de Spectrochimie Infrarouge et Raman CNRS UMR 8516, Bâtiment C5, Université des Sciences et Technologies de Lille, 59655 Villeneuve d'Ascq, France*

 

obtained with density functional theory (DFT) calculations. The geometry optimisation and harmonic frequency calculations have been performed on clusters composed of $Ga(SH)_4$ and $Ga(SH)_3Cl$ subunits. Monomers, CS and ES dimers, CS trimers and tri-clusters have been considered. The assignment of the observed vibrational bands confirms the main structural conclusions obtained with X-ray and neutron diffraction,[12] and gives some new insights into the gallium-network present in the $x$CsCl(1 − $x$)$Ga_2S_3$ glasses.

## Experimental and Computational Methods

### Experimental methods

The glasses were prepared from the base constituents Ga (Aldrich, 99.9995%), S (Aldrich 99.998%), CsCl (Biomol, 99.999%) and sealed in evacuated silica ampoules. A standard tubular oven was used to heat the ampoules, the oven temperature was slowly increased up to 1000 °C. Once homogeneous, the glasses were quenched by water at 20 °C. Compositions of $x$CsCl(1−$x$)$Ga_2S_3$ were synthesised for values of $x = 0.5$, 0.6 and 0.7.

Raman spectra over the spectral range 80–1200 $cm^{-1}$ were taken at room temperature using an LABRAM Dilor spectrometer (Jobin Yvon Horiba Group) equipped with a triple monochromator; liquid nitrogen cooled charge-coupled device (CCD) detector and a microscope. Raman scattering was excited using a 632.8 nm He–Ne laser with a typical power of 1 mW or less. A few spectra were measured for each sample at different positions and with different laser power in order to verify the sample homogeneity and the absence of photo-induced phenomena.

### Computational methods

All calculations were performed using GAUSSIAN 03[13] associated with its graphical user interface GaussView 03. In order to find a compromise between the cost of the calculations and the accuracy of the results, structural optimisations and harmonic vibrational frequency calculations were performed for size-limited clusters composed of $Ga(SH)_4$ and $Ga(SH)_3Cl$ tetrahedral subunits. Concerning the monomers and the ES and CS dimers, the calculations have been performed for both chlorine-doped and undoped structures. For trimers and tri-clusters, the calculations have been limited to clusters without chlorine atoms. In comparison to the study of Grisolía *et al*. 2006 in Ref. [4] where methyl groups were included, hydrogen endings have been used for these calculations. Therefore, calculations on larger clusters with simple or double chlorine substitutions were accessible and the presence of several close minima due to the internal rotation of the methyl groups was avoided. Nevertheless, the assumed tetrahedral environment of the network is more distorted with these endings. Hartree-Fock (HF), DFT and second-order perturbed Møller-Plesset (MP2) level of theory were used for the structure optimisations and frequency calculations of monomers $Ga(SH)_4$ and $Ga(SH)_3Cl$. The presence of several imaginary wavenumbers in the calculations demonstrates that, even for the monomers, the HF method was not suited to efficiently localise the minima of the potential energy surfaces. For dimers and tri-clusters, the semi-empirical DFT calculations were used in preference to the MP2 method because of its lower calculation cost and because the DFT method often gives more conclusive results for the harmonic vibrational frequency determination.[14] All the DFT calculations were performed with the Becke[15] three parameters hybrid exchange functional and the Lee-Yang-Parr correlation functional (B3LYP).[16] All the structures were optimised using the GDIIS convergence criteria ensuring adequate convergence and reliability of computed wavenumbers. Harmonic frequency calculations were performed with the method and basis set used for the optimisation. For the different clusters, several basis sets have been used for the DFT calculations. In the case of clusters without chlorine atoms, the 6-311G+(2d,p) basis set was sufficient to avoid any imaginary wavenumbers which ensures that the optimised structure corresponds to a minimum on the potential energy surface. For chlorine-doped clusters, an extension to the 6-311G+(3df,2p) basis set was required.

## Molecular Structures

X-ray and neutron diffraction experiments have allowed the short-range structure of $x$CsCl(1 − $x$)$Ga_2S_3$ glasses to be analysed.[12] The measurements, performed for $x = 0.5$, 0.6 and 0.7, demonstrated that the structural units are Ga centred tetrahedra composed of a mixed sulfur/chlorine environment. Even for the strongest CsCl concentration, the mean number of gallium–chlorine bond per tetrahedron never exceeds 0.72 which suggests that $GaS_4$ and $GaS_3Cl$ are the most probable subunits expected in these glasses. This study has also shown that sulfur displays a mean coordination of 2.2(1) which indicates the presence of tri-clusters for which sulfur atoms are three-fold coordinated. In agreement with these conclusions, the theoretical analysis, performed in the present work, is focused on monomers, dimers, trimers and tri-clusters composed of $GaS_4$ and the $GaS_3Cl$ tetrahedral subunits. All the studied structures, optimised with the B3LYP method, are shown in Fig. 1.

The average bond distances for these optimised structures are presented in Table 1 and are compared with the theoretical structural analysis in Ref. [14] and the experimental results published in Refs. [10,12] For the optimisation of the monomers $Ga(SH)_4$ and $Ga(SH)_3Cl$, respectively, called $M_1$ and $M_2$ in Fig. 1, the MP2 and B3LYP methods have been used with different basis sets and yielded very close structures with identical bond distances for a tolerance of 1 pm. Therefore, in Table 1, only the bond lengths computed with a B3LYP optimisation are presented. In agreement with the experimental measurements,[12] the presence of chlorine atom induces no variation of the averaged ⟨Ga–S⟩ bond distances which are close to 2.31 Å. The comparison with the calculations on $Ga(SCH_3)_4$ and $Ga(SCH_3)_3Cl$ in Ref. [4] shows that, for clusters with H or $CH_3$ endings, the ⟨Ga–S⟩ bond lengths are identical. Conversely, a noticeable difference is observed for the ⟨Ga–Cl⟩ distance which is smaller in the case of hydrogen endings. For the $M_2$ cluster, the Ga–Cl length is optimised to 2.18 Å which agrees with the estimations deduced from the atomic covalent radii of Cl and S.[10] Table 1 also shows the average bond lengths deduced from the geometry optimisations performed on CS- and ES-bonded dimers, respectively, called Dc and De in Fig. 1. For all the studied dimers, the ⟨Ga–S⟩ bond lengths, calculated with the B3LYP optimisation, are very similar. As for the monomer $M_1$ and $M_2$, the Ga tetrahedral environment (H or $CH_3$ endings, chlorine substitutions) has a weak influence on the ⟨Ga–S⟩ distance and the experimental techniques such as XAS are not able to distinguish such small differences. Similarly, the comparison of the ⟨Ga–S⟩ distances yields no clear conclusion about the ES and the CS nature of the dimers. This observation is also valuable for the ⟨Ga–Cl⟩ distances which are found to be smaller than the ⟨Ga–S⟩ distances, except for the chlorine-connected gallium dimers $D_{c3}$ and $D_{e3}$.

**Table 1.** Averaged ⟨Ga–S⟩, ⟨Ga–Cl⟩ and ⟨Ga–Ga⟩ bond distances obtained in this work with clusters shown in Fig. 1 and in Grisolía *et al.*[4] with $(Ga(SCH_3)_{4-x}Cl_x)_N$ clusters. The theoretical values computed with the B3LYP method are compared with experimental values resulting from X-ray absorption measurements[10,12]

| | ⟨Ga–S⟩ | | ⟨Ga–Cl⟩ | | ⟨Ga–Ga⟩ | |
|---|---|---|---|---|---|---|
| Cluster | This work[a] | Ref. Grisolía *et al.* 2006[b] | This work | Ref. Grisolía *et al.* 2006 | This work | Ref. Grisolía *et al.* 2006 |
| $M_1$ | 2.31 | 2.31 | – | – | – | – |
| $M_2$ | 2.32 | 2.28 | 2.18 | 2.28 | – | – |
| $D_{c1}$ | 2.32 | 2.31 | – | – | 3.35 | 3.92 |
| $D_{e1}$ | 2.31 | 2.32 | – | – | 3.59 | 2.97 |
| $D_{c2}$ | 2.33 | 2.30 | 2.18 | 2.34 | 3.33 | 3.88 |
| $D_{e2}$ | 2.32 | 2.31 | 2.16 | 2.31 | 3.54 | 2.97 |
| $D_{c3}$ | 2.28 | 2.26 | 2.39 | 2.44 | 3.85 | 4.35 |
| $D_{e3}$ | 2.30 | – | 2.42 | – | 2.97 | – |
| $D_{c4}$ | 2.34 | – | 2.18 | – | 3.32 | – |
| $D_{e4}$ | 2.33 | – | 2.16 | – | 3.50 | – |
| $T_1$ | 2.33 | – | – | – | 3.39 | – |
| $T_2$ | 2.30 | – | – | – | 3.89 | – |
| Experimental[c] | 2.28[d] | 2.26[e] | 2.28[d] | 2.20[f] | 3.6(2.9)[g] | 3.5[e] |

[a] Values deduced from the average on each bond length obtained from the optimised structures are shown in Fig. 1.
[b] Averaged bond lengths calculated in Grisolía *et al.*[4] on $(Ga(SCH_3)_{4-x}Cl_x)_N$ clusters using the B3LYP\6-31G** level of theory.
[c] Bond lengths deduced from X-ray and neutron diffraction experiments.
[d] Values deduced from X-ray and neutron measurements in Hindle *et al.*[12]
[e] Values deduced from X-ray absorption spectroscopy in Ramos *et al.*[10]
[f] Values deduced in Hindle *et al.*[12] by taking into account the atomic covalent radii of Cl and S.
[g] 3.6 Å is the length deduced from the Ga–Ga (CS) correlation measurement in Hindle *et al.*[12]; 2.9 Å is the length expected for the Ga–Ga (ES) second nearest neighbour correlation.

Hence, the diffraction data were unable to distinguish between the Ga–S and the Ga–Cl correlations, the calculated differences between the ⟨Ga–S⟩ and ⟨Ga–Cl⟩ bond lengths in this work indicate a possible occurrence of the Ga–Cl bonding in the total correlation functions. The ⟨Ga–Ga⟩ distances, compared in Table 1, show inconsistent results. In this study, the ⟨Ga–Ga⟩ distances of the CS dimers are slightly smaller than the ⟨Ga–Ga⟩ distances of the ES dimers. This observation is not in agreement with Grisolía *et al.*[4] and with extrapolations on $GeS_{4/2}$ data[17] which predict a ⟨Ga–Ga⟩ distance close to 2.9 Å for ES dimers and 3.7 Å for CS dimers. In Ramos *et al.*[10] and Hindle *et al.*[12], these predictions and the absence or the small intensity of correlation peak in the 2.9 Å region indicated that the $GaS_4$ tetrahedral subunits are mostly corner linked in the glass and that the introduction of chlorine atoms does not alter the Ga-based network. Compared with the structures studied in Grisolía *et al.*[4], the tetrahedral subunits with hydrogen endings optimised in this work are more distorted. The calculated ⟨Ga–Ga⟩ distances indicate that the Ga–Ga correlations for CS and ES dimers are both at 3.4 Å which allows the possibility of ES dimers in the network. Finally, except for the chlorine-bonded dimers $D_{c3}$ and $D_{e3}$, the ⟨Ga–Ga⟩ distances are slightly reduced when chlorine atoms are added in the tetrahedral subunits. This conclusion agrees with X-ray and neutron diffraction data previously observed. Table 1 also shows the average ⟨Ga–S⟩ and ⟨Ga–Ga⟩ distances deduced from the optimisations of trimer $T_1$ and tri-cluster $T_2$ in Fig. 1. The DFT calculation predicts a ⟨Ga–Ga⟩ distance close to 3.9 Å, i.e. longer than the ⟨Ga–Ga⟩ distances determined for the dimers and the monomers. Nevertheless, the X-ray and neutron diffraction data around 3.6 Å did not allow the attribution of Ga–Ga correlations to a specific cluster. The calculated differences among the bond lengths ⟨Ga–S⟩, ⟨Ga–Cl⟩ and ⟨Ga–Ga⟩ demonstrate that diffraction measurements may not allow an unambiguous differentiation between the clusters. In particular, several questions remain concerning the size of the clusters and their geometry. In order to examine the details of the clusters present in the glass network, Raman spectroscopy supplemented with harmonic frequency calculations has been employed. In the following sections, the $cm^{-1}$ wavenumber units will be used as the Raman shift units.

## Description of the Experimental Spectra

The experimental Raman spectra of the $x$CsCl$(1-x)Ga_2S_3$ glasses obtained for three different CsCl concentrations $x = 0.5$, 0.6 and 0.7 are represented in Fig. 2.

The strongest vibrational band centred at 320 $cm^{-1}$ has been used to normalise the spectrum of the sample $x = 0.5$. The relative intensities of this band for the two other spectra ($x = 0.6$ and 0.7) have been scaled taking into account the stoichiometry of the $x$CsCl$(1-x)Ga_2S_3$ glasses. The evolution of the Raman spectra with the CsCl concentrations clearly illustrates the deep modifications in the gallium-sulfide network due to the CsCl addition. In the 100–500 $cm^{-1}$ region, the first observation consists on the narrowing of the absorption bands when the CsCl concentration increases. Previous experiments have demonstrated that the metal doping in chalcogenide glasses involves a fragmentation of the glass network into size-limited clusters.[12,17] Therefore, the narrowing of the bands with the addition of CsCl indicates that the narrowest observed peaks may be straightforwardly assigned to a specific molecular vibrational mode of chlorine-doped clusters. In the 200–500 $cm^{-1}$ range, large bands centred at 269 $cm^{-1}$, 320 $cm^{-1}$, 362 $cm^{-1}$ and 404 $cm^{-1}$ are observed to decrease when $x$ increases. Simultaneously, three narrow peaks centred at 253 $cm^{-1}$, 343 $cm^{-1}$ and 400 $cm^{-1}$ appear with the addition of CsCl. In the

Journal of RAMAN SPECTROSCOPY

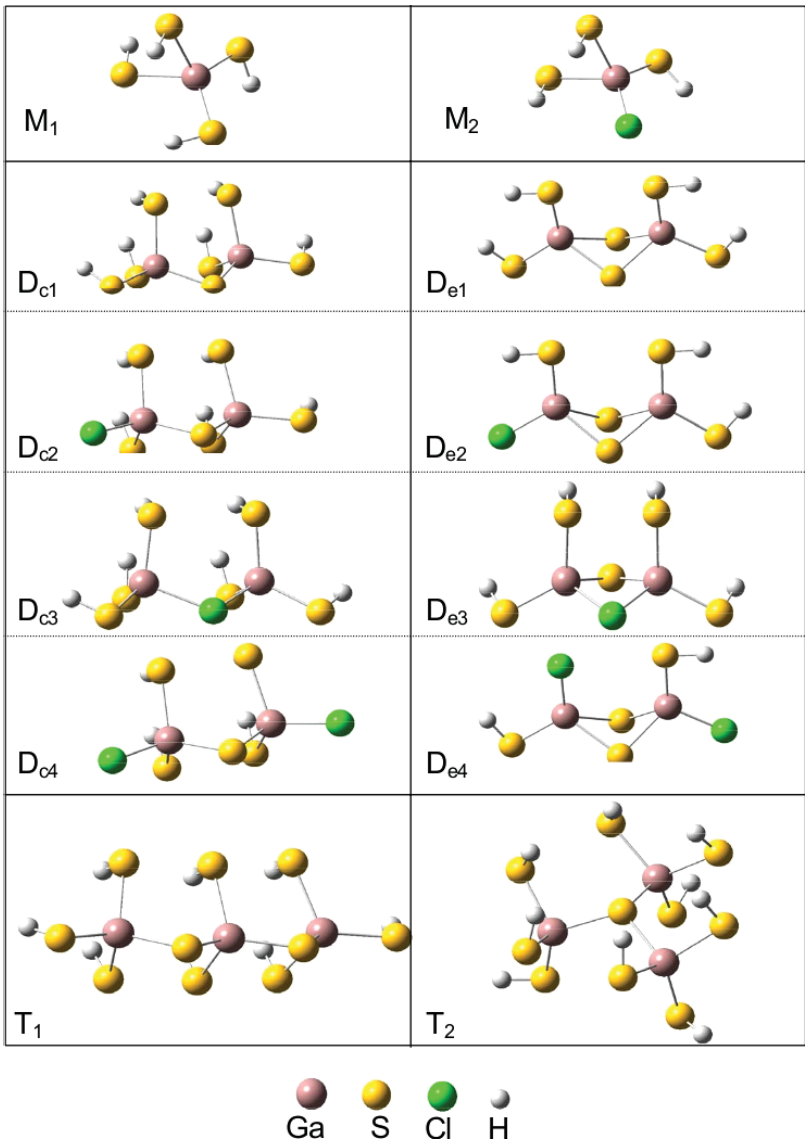


**Figure 1.** Optimised structures with the B3LYP method using the basis sets 6-311G+(2d,p) and 6-311G+(3df,2p) for the clusters without and with chlorine atoms, respectively. $M_1$ and $M_2$ represent the two studied monomers. $D_{c1}$, $D_{c2}$, $D_{c3}$ and $D_{c4}$ represent the studied dimers composed of CS-linked gallium tetrahedral. $D_{e1}$, $D_{e2}$, $D_{e3}$ and $D_{e4}$ represent the studied dimers composed of ES-linked gallium tetrahedral. $T_1$ and $T_2$ represent, respectively, CS trimer and tri-cluster.

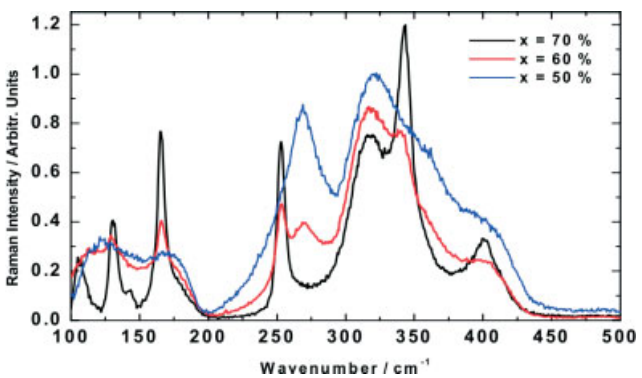


**Figure 2.** Experimental Raman spectra of $x$CsCl(1 − $x$)$Ga_2S_3$ glasses for three different CsCl concentrations: $x$ = 0.7 (black), $x$ = 0.6 (red) and $x$ = 0.5 (blue).

100–200 $cm^{-1}$ spectral region, two broad structures centred at 123 $cm^{-1}$ and 170 $cm^{-1}$ observed for $x$ = 0.5 are replaced by three thin picks centred at 106 $cm^{-1}$, 130 $cm^{-1}$ and 165 $cm^{-1}$ for $x$ = 0.7. In the next section, the glass structure will be investigated by a comparison between the experimental Raman spectra and the theoretical spectra deduced from vibrational harmonic frequencies calculated with the equilibrium structures of the clusters described in Fig. 1. In order to facilitate this comparison, the experimental spectra have been deconvoluted with Gaussians as shown in Fig. 3.

Compared with the Lorentzian profile, the Gaussian band shape was better suited to reproduce the observed vibrational bands and agrees with an assumed inhomogeneous broadening of the vibrational bands. The set of fitted integrated intensities and central wavenumbers allowed each experimental spectrum to be described in form of a stick diagram (*cf* Fig. 3) directly comparable with the theoretical spectra determined by DFT harmonic calculations.



  

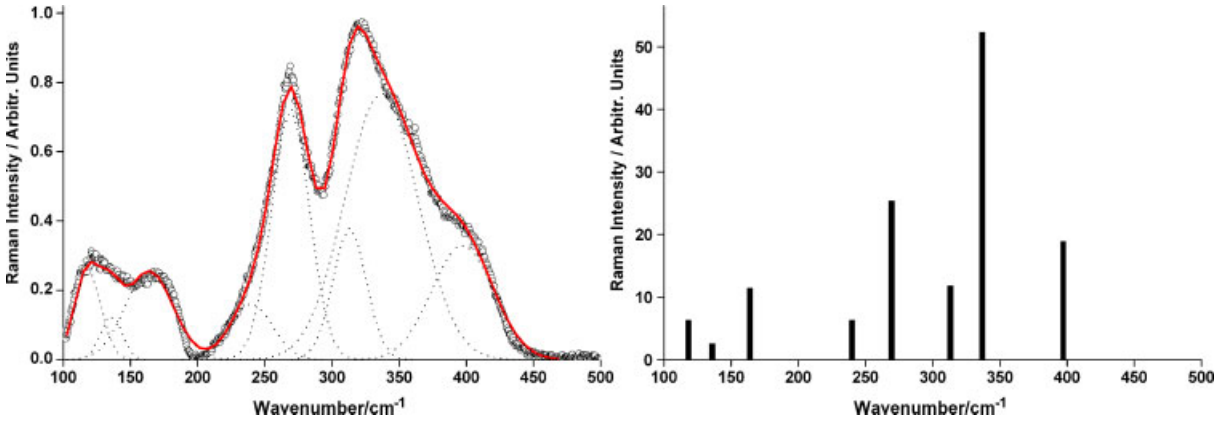


(a) CsCl concentration: $x = 0.5$

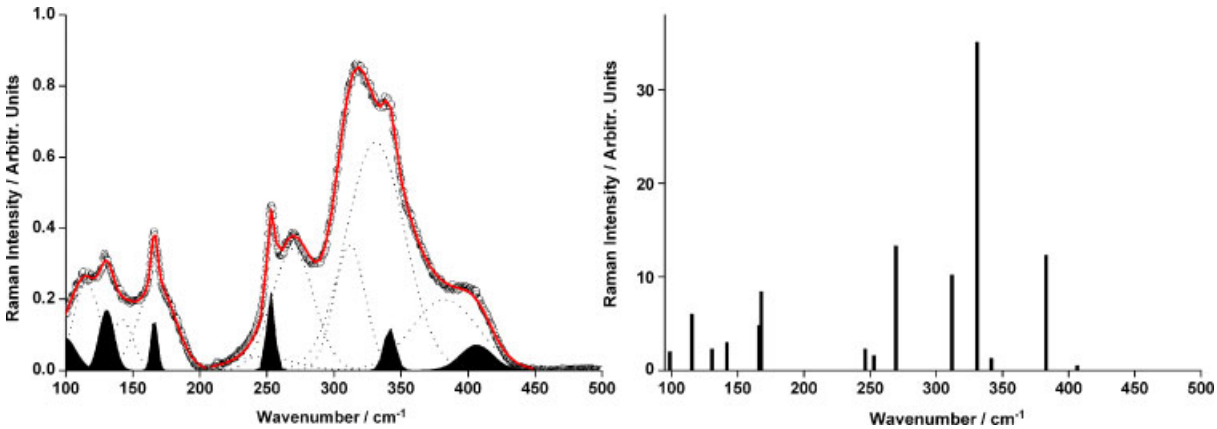


(b) CsCl concentration: $x = 0.6$

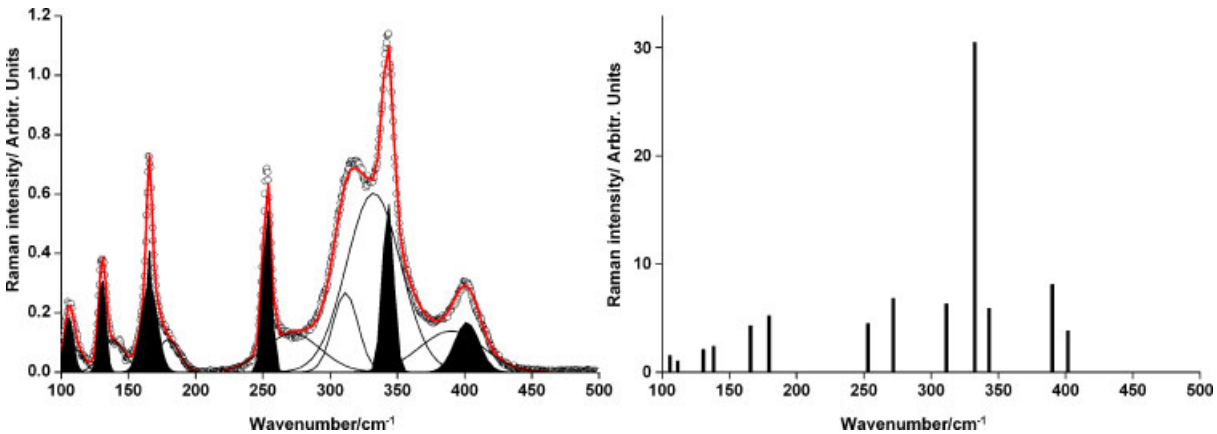


(c) CsCl concentration: $x = 0.7$

**Figure 3.** Left: deconvolution with Gaussian band shapes of experimental Raman spectra of $x$CsCl$(1-x)$Ga$_2$S$_3$ glasses for the three CsCl concentrations: $x = 0.5$ (3-a), $x = 0.6$ (3-b) and $x = 0.7$ (3-c). The narrower vibrational bands which appear with chlorine addition are filled in black. Right: stick diagrams calculated from the wavenumbers and the integrated intensities fitted.

## Vibrational Analysis

### The gallium-sulfide network at low CsCl concentration

In Fig. 3a, the experimental spectrum, obtained for $x = 0.5$, has been fitted using eight Gaussian components. The central wavenumbers and the integrated intensities of these components are listed in Table 2.

Contrary to the spectra obtained with higher CsCl concentrations, the absence of narrow Raman lines suggests that the experimental spectrum of Fig. 3a may be assigned with the vibrational modes belonging to undoped clusters. In Fig. 4, the theoretical spectra obtained with the calculated Raman wavenumbers of the $M_1$, $D_{c1}$, $D_{e1}$, $T_1$ and $T_2$ clusters are presented. The comparison between these theoretical spectra and the measured stick diagram allowed to assign the eight Gaussian components of the measured spectrum to specific vibrational modes of targeted clusters. This assignment is summarised in Table 2 and confirms two important conclusions of the diffraction experiments: Ga tetrahedra are essentially CS and there is a significant proportion of tri-clusters in the network. Indeed, seven components may

**Table 2.** Assignment of the vibrational bands deduced from the deconvolution of the experimental Raman spectra. For $x = 0.5$, the eight Gaussian components of Fig. 3a are assigned with the theoretical spectra of the undoped clusters shown in Fig. 4. For $x = 0.7$, the six Gaussian narrow components which are observed in the spectra 3-b and 3-c are assigned with the theoretical spectra of the Cl-doped clusters shown in Fig. 5

| | | intensity | | wavenumber/cm$^{-1}$ | | | |
|---|---|---|---|---|---|---|---|
| Cluster | Mode description | calc.[a] | obs.[b] | calc. | corr.[c] | obs. | CsCl concentration |
| $T_2$ | Ga–$S_2$ scissoring | 154.3 | w | 111.7 | 111.8 | 118.2 | $x = 0.5$ |
| $D_{c1}$ | Ga–$S_2$ scissoring | 154.6 | | 118.0 | 116.2 | | |
| $T_2$ | Ga–$S_2$ scissoring | 59.0 | vw | 142.8 | 142.9 | 135.8 | |
| $D_{c1}$ | S$Ga_2$ scissoring | 61.2 | | 135.0 | 133.0 | | |
| $T_1$ | Ga–$S_2$ wagging | 454.9 | m | 171.2 | 163.0 | 163.9 | |
| $D_{c1}$ | Ga–$S_2$ wagging | 516.8 | | 164.4 | 161.9 | | |
| $D_{e1}$ | ring out of plane bending | 23.0 | w | 241.9 | 228.5 | 240.0 | |
| $T_1$ | Ga–$S_2$ symmetric stretching | 132.2 | s | 270.1 | 257.2 | 269.3 | |
| $D_{c1}$ | Ga–$S_2$ symmetric stretching | 57.9 | | 262.5 | 258.6 | | |
| $T_2$ | Ga–$S_2$ symmetric stretching | 191.9 | m | 314.8 | 315.1 | 313.1 | |
| $T_1$ | Ga–$S_2$ symmetric stretching | 318.1 | vs | 363.5 | 346.2 | 336.8 | |
| $D_{c1}$ | Ga–S symmetric stretching | 504.5 | | 352.7 | 347.4 | | |
| $D_{e1}$ | Ga–$S_2$ symmetric stretching | 48.1 | | 364.7 | 344.9 | | |
| $T_2$ | Ga–S symmetric stretching | 427.9 | s | 394.4 | 394.8 | 397.2 | |
| $D_{c2}$ | Ga–$S_2$ scissoring | 24.1 | vw | 121.5 | 117.7 | 105.8 | $x = 0.7$ |
| $D_{c3}$ | Ga–$S_2$ twisting | 84.7 | | 103.6 | 101.2 | | |
| $D_{c4}$ | S$Ga_2$ twisting | 12.2 | | 106.9 | 103.0 | | |
| $D_{c2}$ | S$Ga_2$ scissoring | 27.1 | w | 135.3 | 131.1 | 130.6 | |
| $D_{c3}$ | Cl–$Ga_2$ twisting | 490.2 | | 137.9 | 134.7 | | |
| $D_{c4}$ | S–$Ga_2$ twisting | 16.2 | | 136.4 | 131.4 | | |
| $D_{c2}$ | Ga–$S_2$ wagging | 301.4 | w | 183.5 | 177.7 | 165.6 | |
| $D_{c2}$ | Ga–$S_2$ asymmetric stretching | 15.2 | w | 260.8 | 252.6 | 253.0 | |
| $D_{c3}$ | Cl–$Ga_2$ asymmetric stretching | 87.1 | | 250.1 | 244.3 | | |
| $D_{c4}$ | Ga–$S_2$ scissoring | 17.3 | | 259.8 | 250.3 | | |
| $D_{c2}$ | Cl–Ga–S symmetric stretching | 125.6 | w | 365.4 | 353.9 | 343.1 | |
| $D_{c3}$ | Cl–$Ga_2$ symmetric stretching | 1086.4 | | 383.0 | 374.1 | | |
| $D_{c4}$ | S$Ga_2$ asymmetric stretching | 56.7 | | 374.0 | 360.3 | | |
| $D_{c2}$ | Ga–$S_2$ asymmetric stretching | 72.8 | w | 395.2 | 382.8 | 401.8 | |
| $D_{c3}$ | Ga–$S_2$ asymmetric stretching | 2115.8 | | 385.3 | 376.4 | | |
| $D_{c4}$ | Ga–$S_2$ asymmetric stretching | 21.7 | | 402.7 | 388.0 | | |

[a] Raman scattering activities in Å$^4$/amu.
[b] vw, very weak; w, weak; m, medium; s, strong; vs, very strong.
[c] $\nu_{corr} = \lambda \times \nu_{calc}$ with the optimum scaling factors $\lambda$ detailed in Table 3.

be straightforwardly assigned to the vibrational modes deduced from the $D_{c1}$, $T_1$ and $T_2$ calculations. The strongest scattering lines are observed in the 200–450 cm$^{-1}$ range and correspond to Ga–S symmetric stretching modes. Only the Gaussian component centred at 240 cm$^{-1}$ suggests a possible contribution of ES dimers to the vibrational spectra. The presence of tri-clusters $T_2$ with three-fold coordinated sulfur atoms is clearly identified with the two intense spectral lines centred at 313.1 cm$^{-1}$ and 397.2 cm$^{-1}$. In the 100–200 cm$^{-1}$ region, the vibrational bands, mainly assigned to angular deformation modes of the S–Ga–S bonds, indicate the coexistence of CS dimers and tri-clusters in the glass network.

### Chlorine addition in the glass network

The Raman spectrum obtained with the composition $x = 0.6$, shown in Fig. 3b, cannot be fitted using only the eight Gaussian components previously described; it requires six additional components with weaker intensities but narrower bandwidths. These six components are clearly observed in the spectrum 3-c for the highest studied CsCl concentration ($x = 0.7$). With the increasing of the intensities of the six narrow bands, the intensities of all the eight bands, assigned to the vibrational modes of the undoped clusters in the spectrum 3-a, decrease. The Raman experimental data cannot exclude the presence of these six additional components in the spectrum of the $x = 0.5$ sample because their intensity is insufficient to be distinguished from the eight major scattering lines belonging to undoped structural units. The diffraction data, however, unambigously indicate that the $x = 0.5$ sample contains both Cl-doped and undoped tetrahedra.[12] The evolution of the band intensities with the CsCl concentration demonstrates that chlorine atoms replace sulfur atoms in the CS tetrahedral environment. This conclusion agrees with neutron

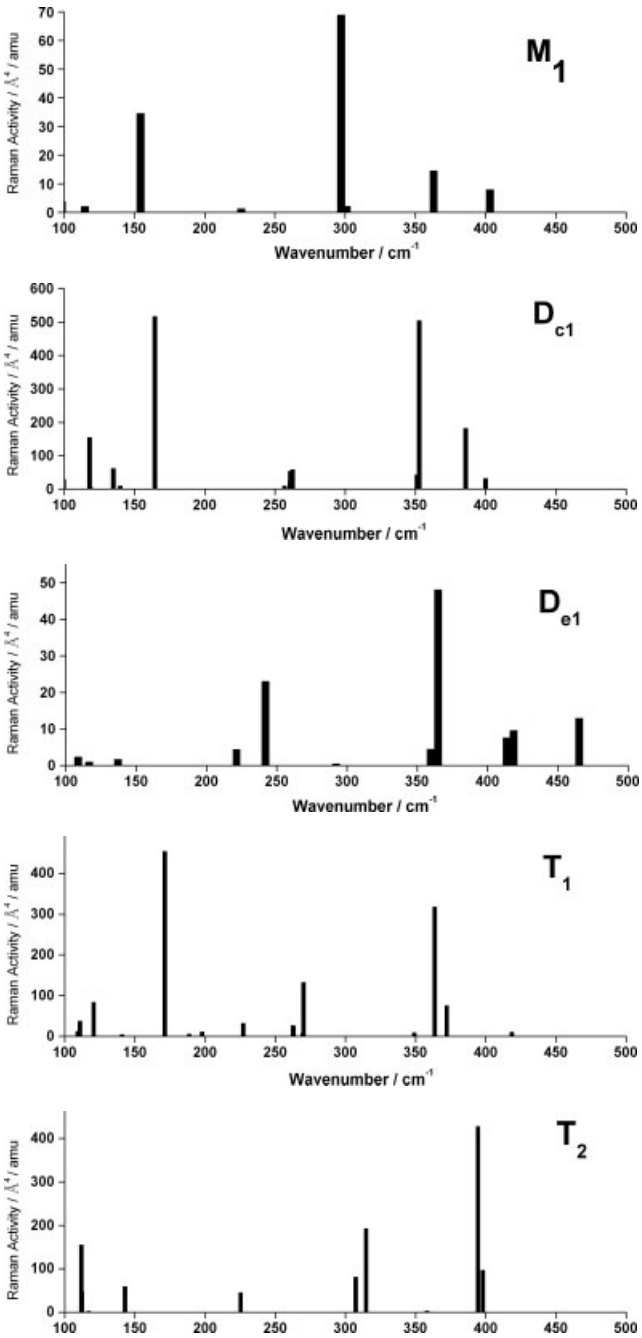


**Figure 4.** B3LYP Raman calculations performed on undoped clusters defined in Fig. 1. The vibrational modes associated with hydrogen endings have been voluntarily removed from these spectra.

diffraction measurements which estimate a number of chlorine bonds per tetrahedron equal to 0.72 at $x = 0.7$.[12] This result and the deconvolution of the spectra 3-b and 3-c demonstrate the coexistence of chlorine-doped and undoped clusters in the glass network. Thanks to DFT calculations, the six narrow bands have been assigned to vibrational modes belonging to chlorine-doped clusters. Figure 5 presents the theoretical spectra of the $M_2$, $D_{c2}$, $D_{c3}$, $D_{c4}$, $D_{e2}$, $D_{e3}$ and $D_{e4}$ clusters. These spectra allowed a vibrational analysis of the six narrow bands, obtained by the deconvolution of the spectra 3-b and 3-c. In the Table 2, the assignment to vibrational modes of chlorine-doped clusters is presented for the spectrum 3-c with $x = 0.7$. In this spectrum, the vibrational band centred at 240 $cm^{-1}$, potentially assignable to ES dimers has completely disappeared, and the chlorine substitutions are predicted in a CS tetrahedral environment described by the three clusters $D_{c2}$, $D_{c3}$ and $D_{c4}$. In Table 2, the vibrational analysis has been performed with the calculated wavenumbers of these three clusters. As for the previously described spectra, two spectral regions may be distinguished by the nature of the vibrational modes: angular deformation modes and stretching modes are, respectively, observed in the 100–200 $cm^{-1}$ and 200–450 $cm^{-1}$ spectral ranges. The theoretical spectra of $D_{c2}$, $D_{c3}$ and $D_{c4}$ predicted different vibrational modes for which the central wavenumbers and the relative intensities matched with

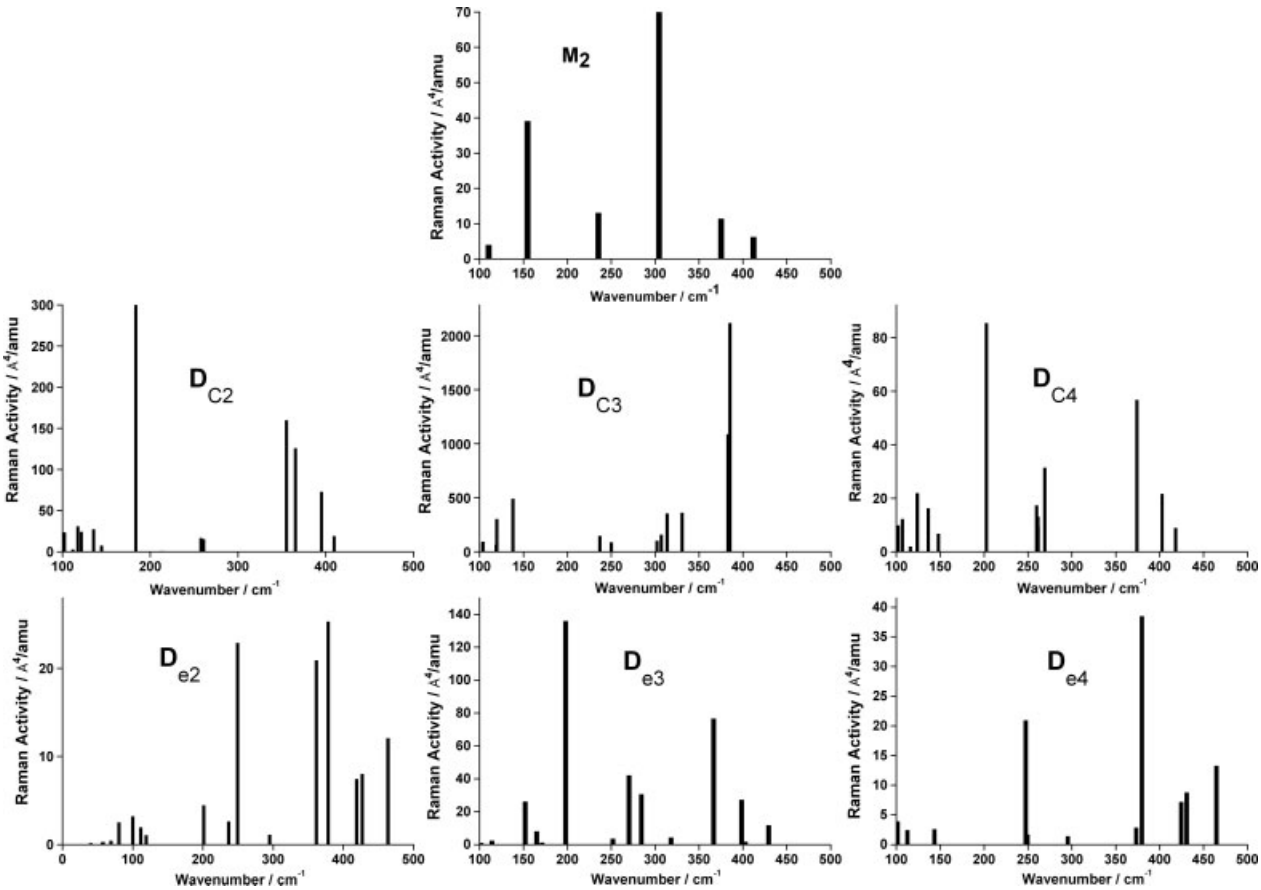


**Figure 5.** B3LYP Raman calculations performed on Cl-doped clusters defined in Fig. 1. The vibrational modes associated with hydrogen endings have been voluntarily removed from these spectra.

the deconvoluted Gaussian components. Therefore, it is difficult to conclude where chlorine atoms are positioned in the corner-shared dimers. However, the fraction of the $D_{c3}$ dimers connecting via bridging Cl species ($N_{Cl-Ga} = 2$) appears to be lower than the $D_{c2}$ and $D_{c4}$ units since the average chlorine coordination number, $N_{Cl-Ga}$, does not exceed 1.[12]

### Vibrational correction factors and quality of the predictions

In order to bring the computed and experimental wavenumbers into better agreement, correction factors may be employed. Optimum scaling factors, defined by $\lambda = \sum_{i=1}^{N}(\nu_{obs,i} \times \nu_{calc,i})/(\nu^2_{calc,i})$ are currently established in order to eliminate known systematic errors in calculated frequencies.[18] In this study, the optimum scaling factors have been calculated by summations on all assigned normal modes. Owing to the lack of observed vibrational bands, an analysis taking into account each family of normal modes could not be performed. The optimum scaling factors determined for each of the identified clusters are presented in Table 3.

The values, all of which lie the range 0.94447–1.00103, confirm that the theoretical calculations of harmonic frequencies of small clusters with the B3LYP method is well adapted for the vibrational analysis of $x$CsCl(1 − $x$)$Ga_2S_3$ glasses. From these optimum scaling factors, the corrected wavenumbers, defined by $\nu_{corr,i} = \lambda \times \nu_{calc,i}$, are listed in Table 2. In the majority of the cases, the global scaling correction improves the agreement between computed and observed wavenumbers. The quality of the prediction may be also indicated by the root-mean-square standard deviation,

$$\sigma = \sqrt{\sum_{i=1}^{N}(\lambda \times \nu_{calc,i} - \nu_{obs,i})^2}$$

**Table 3.** Optimum scaling factors λ and quality of the wavenumber predictions evaluated with the root-mean-square standard deviation σ for each identified clusters

| Cluster | $N$[a] | λ[b] | σ[c] /cm$^{-1}$ | Level of theory |
|---|---|---|---|---|
| $D_{c1}$ | 4 | 0.98505 | 7.0 | B3LYP/6-311G+(2d,p) |
| $D_{e1}$ | 2 | 0.94447 | 9.8 | |
| $T_1$ | 3 | 0.95234 | 8.8 | |
| $T_2$ | 4 | 1.00103 | 5.0 | |
| $D_{c2}$ | 6 | 0.96866 | 12.4 | B3LYP/6-311G+(3df,2p) |
| $D_{c3}$ | 5 | 0.97683 | 18.6 | |
| $D_{c4}$ | 5 | 0.96347 | 10.0 | |

[a] $N$ corresponds to the number of calculated wavenumbers.
[b] λ is the optimum scaling factors defined by $\lambda = \sum_{i=1}^{N}(\nu_{obs,i} \times \nu_{calc,i})/(\nu^2_{calc,i})$.
[c] σ is the root-mean-square standard deviation defined by:

$$\sigma = \sqrt{\sum_{i=1}^{N}(\lambda \times \nu_{calc,i} - \nu_{obs,i})^2}.$$

where $N$ is the number of assigned normal modes. The $\sigma$ values, presented in Table 3 for each cluster, are in the range 5–9.8 $cm^{-1}$ for undoped clusters and 10–18.6 $cm^{-1}$ for chlorine-doped clusters. Finally, it is noteworthy that the highest $\sigma$ value is obtained for the chlorine-bonded $D_{c3}$ dimer which cast a doubt on the possibility of chlorine-bonded dimers and suggests that chlorine atoms are mainly terminal in the corner-shared dimers.

## Conclusion

The Raman spectra of $x$CsCl$(1-x)Ga_2S_3$ glasses, obtained for three different CsCl concentrations ($x = 0.5$, 0.6 and 0.7) have been analysed using DFT harmonic frequency calculations on specific clusters composed of $GaS_4H_4$ and/or $GaS_3H_3Cl$ tetrahedral subunits. The assignment of the observed vibrational bands confirms the main structural conclusions obtained with X-ray and neutron diffraction experiments[9] and gives some new insights into the gallium-network present in the $x$CsCl$(1-x)Ga_2S_3$ glasses. At the lowest concentration ($x = 0.5$), the observed bands have been assigned to the vibrational modes belonging to undoped clusters. The comparison with the predicted spectra demonstrated a coexistence of dimers and tri-clusters in the glass. The dimers are essentially connected by CS tetrahedra in the network and the ES dimers completely disappear at higher CsCl concentrations. A significant proportion of tri-clusters with three-fold coordinated sulfur atoms has been identified. For higher CsCl concentrations ($x = 0.6$ and 0.7), a fragmentation of the glass network is expected with the addition of chlorine atoms which replace the sulfur atoms in the CS tetrahedral environment. Nevertheless, undoped and chlorine-doped clusters coexist in the glass over the whole composition range from $x = 0.5$ to 0.7. It is difficult to determine the precise chlorine sites but the agreement between computed and observed wavenumbers favoured a terminal position of the chlorine atoms in the CS dimers ($N_{Cl-Ga} = 1$) over chlorine-bonded dimers ($N_{Cl-Ga} = 2$). This study could be completed using a theoretical approach by the improvement of the quality of the predictions using advanced DFT methods[19] including anharmonic force fields calculations[20] and by an extension of the calculations to more complex clusters such as chlorine-doped tri-clusters. Finally, a complete vibrational analysis should be obtained with additional infrared experiments on $x$CsCl$(1-x)Ga_2S_3$ glasses.

### Acknowledgement

The part of this work was supported by the European commission within the framework of the Interreg IIIA programme (CTMM2 project).

## References

[1] B. G. Aitken, R. S. Quimby, *J. Non-Cryst. Solids* **1997**, *213*, 281.
[2] J. R. Hector, J. Wang, D. Brady, M. Kluth, D. W. Hewak, W. S. Brocklesby, D. N. Payne, *J. Non-Cryst. Solids* **1998**, *239*, 176.
[3] S. Griscom, R. Balda, A. Mendioroz, F. Smektala, J. Fernandez, J. L. Adam, *J. Non-Cryst. Solids* **2001**, *284*, 268.
[4] M. Grisolía, L. Rincon, R. Almeida, *J. Mol. Struct (Theochem)* **2006**, *769*, 143.
[5] J. O. Jensen, D. Zeroka, *J. Mol. Struct (Theochem)* **2000**, *505*, 31.
[6] J. O. Jensen, D. Zeroka, *J. Mol. Struct (Theochem)* **1999**, *487*, 267.
[7] H. A. Kassim, I. A. Jalil, N. Yusof, V. Radhika Devi, K. N. Shrivastava, *J. Non-Cryst. Solids* **2007**, *353*, 111.
[8] S. Rada, E. Cuela, M. Bosca, M. Cuela, R. Muntean, P. Pascuta, *Vib. Spectrosc.* **2008**, *48*, 285.
[9] P. Boolchand, M. Jin, D. I. Novita, S. Chakravarty, *J. Raman Spectrosc.* **2007**, *38*, 660.
[10] A. Y. Ramos, M. Grisolía Cardona, H. C. N. Tolentino, M. C. M. Alves, N. Watanabe, O. L. Alves, L. C. Barbosa, *J. Mater. Res.* **2001**, *16*, 1349.
[11] A. Tverjanovich, Y. S. Tveryanovich, S. Loheider, *J. Non-Cryst. Solids* **1996**, *208*, 49.
[12] F. Hindle, M. Miloshova, E. Bychkov, C. J. Benmore, A. C. Hannon, *J. Non-Cryst. Solids* **2008**, *354*, 134.
[13] M. J. Frisch, G. W. Trucks, H. B. Schlegel, G. E. Scuseria, M. A. Robb, J. R. Cheeseman, J. A. Montgomery Jr., T. Vreven, K. N. Kudin, J. C. Burant, J. M. Millam, S. S. Iyengar, J. Tomasi, V. Barone, B. Mennucci, M. Cossi, G. Scalmani, N. Rega, G. A. Petersson, H. Nakatsuji, M. Hada, M. Ehara, K. Toyota, R. Fukuda, J. Hasegawa, M. Ishida, T. Nakajima, Y. Honda, O. Kitao, H. Nakai, M. Klene, X. Li, J. E. Knox, H. P. Hratchian, J. B. Cross, C. Adamo, J. Jaramillo, R. Gomperts, R. E. Stratmann, O. Yazyev, A. J. Austin, R. C. Cammi, Pomelli, J. W. Ochterski, P. Y. Ayala, K. Morokuma, G. A. Voth, P. Salvador, J. J. Dannenberg, V. G. Zakrzewski, S. Dapprich, A. D. Daniels, M. C. Strain, O. Farkas, D. K. Malick, A. D. Rabuck, K. Raghavachari, J. B. Foresman, J. V. Ortiz, Q. Cui, A. G. Baboul, S. Clifford, J. Cioslowski, B. B. Stefanov, G. Liu, A. Liashenko, P. Piskorz, I. Komaromi, R. L. Martin, D. J. Fox, T. Keith, M. A. Al-Laham, C. Y. Peng, A. Nanayakkara, M. Challacombe, P. M. W. Gill, B. Johnson, W. Chen, M. W. Wong, C. Gonzalez, J. A. Pople, *Gaussian 03, Revision B. 04*, Gaussian, Inc.: Pittsburgh, PA, **2003**.
[14] A. Cuisset, G. Mouret, O. Pirali, P. Roy, F. Cazier, H. Nouali, J. Demaison, *J. Phys. Chem. B* **2008**, *112*, 12516.
[15] A. D. Becke, *J. Chem. Phys.* **1993**, *98*, 5648.
[16] C. Lee, W. Yang, R. G. Parr, *Phys. Rev. B.* **1988**, *37*, 785.
[17] E. Bychkov, D. L. Price, A. Lapp, *J. Non-Cryst. Solids* **2001**, *293*, 211.
[18] M. W. Wong, *Chem. Phys. Lett.* **1996**, *256*, 391.
[19] R. Marchal, P. Carbonnière, D. Begue, C. Pouchan, *Chem. Phys. Lett.* **2008**, *453*, 49.
[20] P. Carbonnière, C. Pouchan, *Chem. Phys. Lett.* **2008**, *462*, 169.